British Journal of Pharmacology (2000) 129, 991–999

www.nature.com/bjp

Pharmacological characterization of small-conductance Ca^{2+}-activated K^+ channels stably expressed in HEK 293 cells

[1]Dorte Strøbæk, [1]Tino D. Jørgensen, [1]Palle Christophersen, [1]Philip K. Ahring & *,[1]Søren-Peter Olesen

[1]NeuroSearch A/S, 93 Pederstrupvej, DK-2750 Ballerup, Denmark

1 Three genes encode the small-conductance Ca^{2+}-activated K^+ channels (SK channels). We have stably expressed hSK1 and rSK2 in HEK 293 cells and addressed the pharmacology of these subtypes using whole-cell patch clamp recordings.

2 The bee venom peptide apamin blocked hSK1 as well as rSK2 with IC_{50} values of 3.3 nM and 83 pM, respectively.

3 The pharmacological separation between the subtypes was even more prominent when applying the scorpion peptide blocker scyllatoxin, which blocked hSK1 with an IC_{50} value of 80 nM and rSK2 at 287 pM.

4 The potent small molecule blockers showed little differentiation between the channel subtypes. The bis-quinolinium cyclophane UCL 1684 blocked hSK1 with an IC_{50} value of 762 pM and rSK2 at 364 pM. The antiseptic compound dequalinium chloride blocked hSK1 and rSK2 with IC_{50} values of 444 nM and 162 nM, respectively.

5 The nicotinic acetylcholine receptor antagonist d-tubocurarine was found to block hSK1 and rSK2 with IC_{50} values of 27 μM and 17 μM when measured at +80 mV. The inhibition by d-tubocurarine was voltage-dependent with increasing affinities at more hyperpolarized potentials.

6 The $GABA_A$ receptor antagonist bicuculline methiodide also blocked hSK1 and rSK2 in a voltage-dependent manner with IC_{50} values of 15 and 25 μM when measured at +80 mV.

7 In conclusion, the pharmacological separation between SK channel subtypes expressed in mammalian cells is too small to support the notion that the apamin-insensitive afterhyperpolarization of neurones is mediated by hSK1.

British Journal of Pharmacology (2000) **129,** 991–999

Keywords: Calcium-activated potassium channel; SK; HEK 293; apamin; scyllatoxin; d-tubocurarine; UCL 1684; dequalinium chloride; bicuculline methiodide; taicatoxin

Abbreviations: AHP, afterhyperpolarization; BK, large-conductance Ca^{2+}-activated K^+ channel; CHO cells, Chinese hamster ovary cells; HEK 293 cells, human embryonic kidney cells; IK, intermediate-conductance Ca^{2+}-activated K^+ channel; mAHP, medium afterhyperpolarization; sAHP, slow afterhyperpolarization; SK, small-conductance Ca^{2+}-activated K^+ channel; UCL 1684, 17,24-diaza-1,9-diazoniaheptacyclo[23.6.2.$2^{9,16}$.$2^{19,22}$.$1^{3,7}$.$0^{10,15}$.$0^{26,31}$]octatriaconta-1(32), 3,5,7(38),9,11,13,15,19,21,25(33),26,28,30,34,36-hexadecaene bis(trifluoroacetate)

Introduction

Small-conductance Ca^{2+}-activated K^+ channels (SK channels) belong to a group of Ca^{2+}-activated K^+ channels which is constituted by three major subfamilies named after their single channel conductance: SK, IK, and BK channels, referring to Small, Intermediate and Big conductance (for a recent review see Vergara *et al*., 1998). SK channels were first identified in cultured rat skeletal muscles (Blatz & Magleby, 1986) and shown to be the receptor for the bee venom peptide apamin. Apamin is a selective SK channel blocker that has been reported to cross the blood brain barrier (Habermann, 1984; Messier *et al*., 1991). Apamin has therefore been widely used as the tool to address the presence and function of SK channels in peripheral tissues as well as in the CNS.

The increase in intracellular calcium following action potentials can activate several types of Ca^{2+}-activated K^+ channels leading to an afterhyperpolarization (AHP) of the neurone. In hippocampal pyramidal cells (Stocker *et al*., 1999) and autonomic and cortical neurones (Sah & McLachlan, 1991; Schwindt *et al*., 1988) the AHP has several temporal phases each with a distinct pharmacology (for a review see Sah, 1996). A fast AHP is mediated by charybdotoxin-sensitive BK channels (Pennefather *et al*., 1985; Storm, 1987) and participate in the repolarization of an action potential. Activation of apamin-sensitive SK channels generates an AHP of medium duration (100–200 ms, mAHP) that closely follows the increase and decrease in intracellular Ca^{2+} (Pennefather *et al*., 1985; Sah & Clements, 1999). The mAHP can be followed by a slow AHP (sAHP) lasting several seconds. No pharmacological modulators has been attributed to Ca^{2+}-activated K^+ channels underlying the sAHP's, however they can be modulated by a range of neurotransmitters (Schwindt *et al*., 1992; Pedarzani & Storm, 1993). The single channel conductance of the channels underlying the sAHP has been estimated to 6.8 pS by noise analysis (Sah, 1995) and it has been suggested that apamin-insensitive SK channels mediate the sAHP (Köhler *et al*., 1996). The apamin-sensitive mAHP serve to set the frequency of action potential firing whereas activation of the apamin-resistant sAHP leads to spike-frequency adaptation (Sah, 1996; Stocker *et al*., 1999). Three closely related SK channel subtypes denoted SK1, SK2, and SK3 have been cloned (Köhler *et al*., 1996). They are 70–80% identical at the amino acid level and share some homology to the IK channels (40–50%) whereas the homology to BK

*Author for correspondence; E-mail: SPO@neurosearch.dk

channels is very small (<15%). When these channels were expressed in *Xenopus* oocytes, an apamin-sensitivity in the picomolar range (IC_{50} = 63 pM) was found for rSK2. hSK1 was insensitive to 100 nM apamin whereas an intermediate sensitivity (IC_{50} = 2 nM) was found for rSK3 (Köhler *et al*., 1996; Ishii *et al*., 1997). Based on these findings it was suggested that apamin-insensitive SK1 subunits generate the apamin-resistant sAHP, whereas SK2-3 probably underlie the apamin-sensitive AHPs.

While apamin is the classical blocker of SK channels, several other compounds have been shown to block the apamin-sensitive SK channels or AHPs. Among these are the scorpion peptide scyllatoxin (Chicchi *et al*., 1988; Auguste *et al*., 1990; Hanselmann & Grissmer, 1996; Stocker *et al*., 1999), the plant alkaloid d-tubocurarine (Nohmi & Kuba, 1984; Goh & Pennefather, 1987; Stocker *et al*., 1999), and lately the water-soluble analogues of the $GABA_A$ receptor antagonist bicuculline (Johnson & Seutin, 1997; Debarbieux *et al*., 1998; Stocker *et al*., 1999). The antiseptic compound dequalinium chloride was described as a SK channel blocker (Castle *et al*., 1993; Dunn, 1994), and has constituted a lead for several new SK channel blockers with the bis-quinolinium cyclophane, UCL 1684, being the most potent so far (Campos-Rosa *et al*., 1998).

Most pharmacological data for SK channels have been obtained on cultured cells or tissues, with unknown subunit identity of the channels underlying the current. From the studies on cloned SK1 and SK2 channels expressed in *Xenopus* oocytes only limited pharmacological data has been reported. We here report a broad pharmacological profile of cloned SK1 and SK2 channels. The effects of various peptides including apamin and small molecule blockers claimed to inhibit SK channels or AHPs in native cells were characterized on hSK1 and rSK2 channels stably expressed in HEK 293 cells.

Methods

Plasmid constructs

hSK1 and rSK2 were cloned as follows. Human hippocampus $polyA^+$ mRNA and rat brain $polyA^+$ mRNA (Clontech) was reverse transcribed using Superscript (Life Technologies) according to manufacturer's instructions. Twenty-five ng human first strand cDNA or 100 ng rat first strand cDNA was used as template for PCR using 0.5 μM of gene specific primers and Expand HF polymerase (Boehringer). For rSK2 four fragments covering the entire open reading frame were amplified and cloned into pCRscript (Stratagene). For hSK1 the PCR amplifications yielded two fragments covering only 937 of the 1686 total base pairs. The remaining 749 base pairs were made synthetically and all fragments were cloned into pCRscript. Following sequencing, fragments were excised using restriction enzymes and pieced together to give two full length clones. Following subcloning the full length clones were resequenced.

The full length hSK1 protein sequence was found to be; MPGPRAACSEPNPCTQV VMNSHSYNGSVGRPLGSGP-GALGR DPPDPEA GHPPQPPHSP GLQV VVAKSEPARP-SPGSP RGQP QDQD DDEDDEEDEAGRQRASGKPSNV-GHRLG HRRALFE KRKRLSD YALIFGMFGIVVMVTE-TELSW GVY TKESL YSFAL KCLISL STAILLGLVVLYH-AREIQ LFMV DNG ADDW RIA MTC ERV FLI SLE LAV-CAIH PVP GHY RFT WTA RLA FTYAPSVAEADVDVLL-SIPM FLRLY LLGRV MLLHS KIFT DASSRSIGALNKIT-FNT RFVMK TLMTIC PGTVLLVFSISSWIIAAWTVRVC-ERYH DKQE VTSN FLGA MWLI SITF LSIG YGDMVPH-TYCGKGVCLLTGIMGAGCTA LVV AVVA RKLELTKA-EKHV HNFM MDTQLTKRVKNAAANVLRETWLIYKH-TRLV KKPDQ ARVR KHQR KFLQAIHQAQKLRSVKIE-QGKLND QANTLT DLAK TQT VMYD LVSELHAQHEE-LEARL ATLES RLDALGASLQALPGLIAQAIRPPPPPLP-PRPGPGPQDQAARSSPCRWTPVAPSDCG, which is 100% identical to the sequence by Köhler *et al*. (1996) (GenBank accession U69883). The bases in the synthetic parts of hSK1 were designed with modifications from those of GenBank accession U69883, but they are translated into the same full length sequence. The full length sequence of rSK2 is identical to GenBank accession U69882. The hSK1 and rSK2 clones were then subcloned into pNS1z (a NeuroSearch custom made expression vector derived from pcDNA3 (In Vitrogen) using zeocin as selection marker).

Cell culture and stable transfections

HEK 293 (ATCC CRL-1573) cells were cultured in DMEM medium supplemented with 10% foetal calf serum and 2 mM Glutamax (Gibco, BRL). The cells were grown at 37°C in a humidified atmosphere of 5% CO_2 and 95% air. Cells cultured to 50–60% confluency in a T25 flask (Nunc) were transfected with 2.5 μg expression plasmid using lipofectamine (Gibco, BRL) according to manufacturer's instructions. Transfected cells were selected in medium supplemented with 0.25 mg ml^{-1} Zeocin. Single clones were picked and propagated in selection media until sufficient cells were available for freezing, thereafter the cells were cultured in regular media without a selection agent. Expression of functional hSK1 and rSK2 channels were verified by patch-clamp measurements.

Electrophysiology

All experiments were performed in the patch clamp whole-cell mode. Coverslips (3.5 mm) containing SK expressing HEK 293 cells were transferred to a 15 μl recording chamber and perfused with saline at a rate of 1 ml min^{-1} (~1 volume s^{-1}). Pipettes were pulled from borosilicate glass (Modulohm, Denmark) with a DPZ electrode puller (Zeitz Instruments, Germany) and placed in an electrode-holder at the headstage of an EPC-9 amplifier (HEKA electronics, Germany). The EPC-9 amplifier was connected to a Macintosh G3 computer *via* an ITC-16 interface. Data was sampled with Pulse software (HEKA electronics, Germany) and analysed with IGOR (WaveMetrics, Lake Oswego, OR, U.S.A.). The pipettes had a resistance of 1.8–3 MΩ when filled with intracellular solution and the electrodes were zeroed just before touching a cell. Capacitative transients were automatically cancelled after establishment of the gigaseal, and again after entering the whole-cell mode. The series resistance's recorded after breakthrough to the whole-cell mode were in the range 3–5 MΩ. The series resistance was compensated 80%, updated between sweeps, and never exceeded 8 MΩ. Currents were recorded after application of voltage ramps from −80 to +80 mV (200 ms duration, applied every 5 s). In the determination of reversal potentials with physiological ion gradients the ramps went from −100 to +100 mV. Two extracellular salines were used. One contained (in mM): KCl 144, $CaCl_2$ 2, $MgCl_2$ 1 and HEPES 10 with pH adjusted to 7.4 before use. In the second 144 mM KCl was replaced with 4 mM KCl and 140 mM NaCl. The intracellular solutions used in the pipettes contained 150 mM KCl, 10 mM HEPES (pH was adjusted to 7.2 before use), and 10 mM EGTA as well as

$CaCl_2$ and $MgCl_2$ in concentrations calculated (EqCal, Cambridge, U.K.) to result in free concentrations of 100–300 nM for $CaCl_2$ and 1 mM for $MgCl_2$. Peptides were dissolved in extracellular K^+ saline containing 0.1% BSA and diluted in this saline containing 0.01% BSA. All solutions contained 0.01% BSA in experiments where peptides were used. Dequalinium chloride was dissolved in methanol and the remaining organic blockers were dissolved in DMSO as 1000 fold stock solutions that were diluted in the extracellular saline.

HEK 293 cells express small endogenous currents, which could only be discerned when the internal Ca^{2+} concentration was below 100 nM. A voltage-activated K^+ current with an activation threshold of −20 mV (measured from tail-current analysis, not shown) was initially present in approximately 15% of the cells. The mean value for this current was 75 pA at +80 mV for both cell lines. The holding potential of 0 mV used in the experiments induced a time-dependent inactivation of this current. In 40% of the cells an endogenous inward current was recorded at negative potentials. The mean amplitude of this current was −100 pA measured at −80 mV. These endogenous currents implicate that the potency of the drugs might be slightly underestimated as no correction for leak or background currents was performed and in all fitting procedures 100% blockage was set to zero current.

For most of the compounds a full dose-response experiment (5–9 concentrations) was first performed to get an estimate of the IC_{50} value and to calculate the Hill-coefficient. Then, the compounds were tested 3–5 times at a single concentration to obtain k_{on} and k_{off}, and an IC_{50} value based on these. Data are presented as mean± s.e.mean of n experiments. The IC_{50} values were calculated at −80 mV and at +80 mV in order to address if the block showed any voltage-dependency.

Fitting procedures

IC_{50} values were either calculated from cumulative, equilibrium dose-response experiments or from single-addition, non-equilibrium experiments by an estimate of the kinetic parameters for the block. Normalized data from the dose-response experiments were fitted to a Hill-equation:

$$\frac{I_c}{I_0} = 1 - \frac{C^n}{C^n + K_I} \quad (1)$$

where I_0 is the unblocked current level, I_C is the stationary current level at the concentration C, K_I is the inhibitory constant for the blocker reaction and n is the Hill coefficient. For the compounds tested in this study n was 1, indicating that the blocker/channel reactions obey simple Michaelis-Menten type kinetics.

In the kinetic approach the blocker-induced decrease in current vs time was fitted to the non-equilibrium version of the Michaelis-Menten equation:

$$I_t = I_0 \left(1 - \left(\frac{C}{C + K_I} \cdot \left(1 - \exp^{-t(C \cdot k_{on} + k_{off})}\right)\right)\right) \quad (2)$$

where k_{off} is the off-rate (in s^{-1}), k_{on} is the on-rate (in $M^{-1} \cdot s^{-1}$), $K_I = k_{off} \cdot k_{on}^{-1}$ is the inhibitory constant, I_0 is the current at time 0 (the basic, unblocked current), t is the time after addition of compound at the concentration C.

The blocker potencies are given as IC_{50} values which equal K_I in the case of Michaelis-Menten kinetics. For both methods the fitting routines were written in IGOR software.

Drugs

Apamin and taicatoxin was obtained from Alomone Labs. Charybdotoxin, dequalinium chloride, and BSA were purchased from SIGMA. Scyllatoxin was from BACHEM. D-tubocurarine pentahydrate and EGTA was from Fluka. Bicuculline methiodide was from Research Biochemicals International and UCL 1684 was synthesized at NeuroSearch after patent no. WO 97/48705 by Campos-Rosa *et al.* (1997).

Results

Basic characteristics of the hSK1 and rSK2 expressing HEK 293 cells

Figure 1 shows the IV curves obtained by application of voltage ramps to hSK1 and rSK2 expressing cell lines. SK currents were seen as inwardly rectifying currents developing slowly after breakthrough to the whole-cell configuration. For hSK1 the currents reversed at −81±2.3 mV with 4 mM K^+ and at 0.1±0.4 mV (n=6) with a 144 mM K^+ solution in the bath. For rSK2 the reversal potentials were −85±2.4 mV and 0.6±0.3 mV (n=7) consistent with expression of K^+ selective currents. All of the following experiments were performed with the 144 mM K^+ solution in the bath.

The SK currents were activated by the pipette solution having free Ca^{2+} buffered to 185 or 220 nM. At Ca^{2+} concentrations below 100 nM the SK currents were small (<50 pA), and at a Ca^{2+} concentration in the pipette of

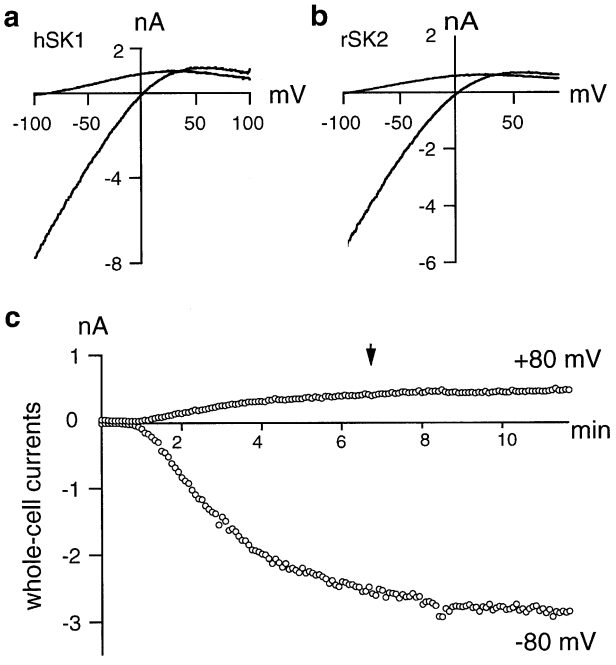

Figure 1 Current-voltage relations and Ca^{2+}-dependent activation of whole-cell SK currents. The whole-cell currents recorded after application of voltage-ramps (−100 to +100 mV, 200 ms duration) to the SK expressing HEK 293 cell lines are shown as a function of the ramp potential for a hSK1 expressing cell (a) and a rSK2 expressing cell (b). The two traces in each panel were obtained with 140 mM Na^+ plus 4 mM K^+ or with 144 mM K^+ in the bath solutions. (c) is the current at −80 mV and at +80 mV measured from voltage ramps applied to a hSK1 expressing cell and plotted as a function of time. The arrow indicates the time at which an experiment would normally start.

300 nM the currents activated faster and often exceeded −10 nA at −80 mV. Activation of SK currents typically displayed three temporal phases as illustrated in Figure 1c.

Table 1 Characterization of the hSK1 and rSK2 expressing HEK 293 cell lines

	Cell size (pF)	*pA pF^{-1} at −80 mV*	*pA pF^{-1} at +80 mV*	$\frac{I_{-80mV}}{I_{+80mV}}$	n
hSK1	9.3±0.59	273±39	55±9.4	5.5±0.25	19
rSK2	11±1.1	288±34	50±7.2	6.1±0.36	13

The values were obtained 5 min after obtaining the whole-cell configuration in experiments with 185 nM free calcium in the pipette solution.

During the first few sweeps SK currents were insignificant but after 10–100 s the small (<50 pA) linear leak current was replaced by an inwardly rectifying current. The currents increased rapidly during the next couple of minutes with a similar shape of the IV (ramp) currents from the first signs until the quasi-stable level was obtained. This increase was presumably due to dilution of the cytosol by a pipette solution with an elevated free Ca^{2+} concentration. After this fast increase in whole-cell current a slower increase was observed. The slow increase often proceeded for more than 30 min, which is far beyond the time expected for exchange of the cytosol by the pipette solution. The reason for this continued increase (run-up) in the current is not clear, but was not caused by an increase in leak-currents since the currents could be fully

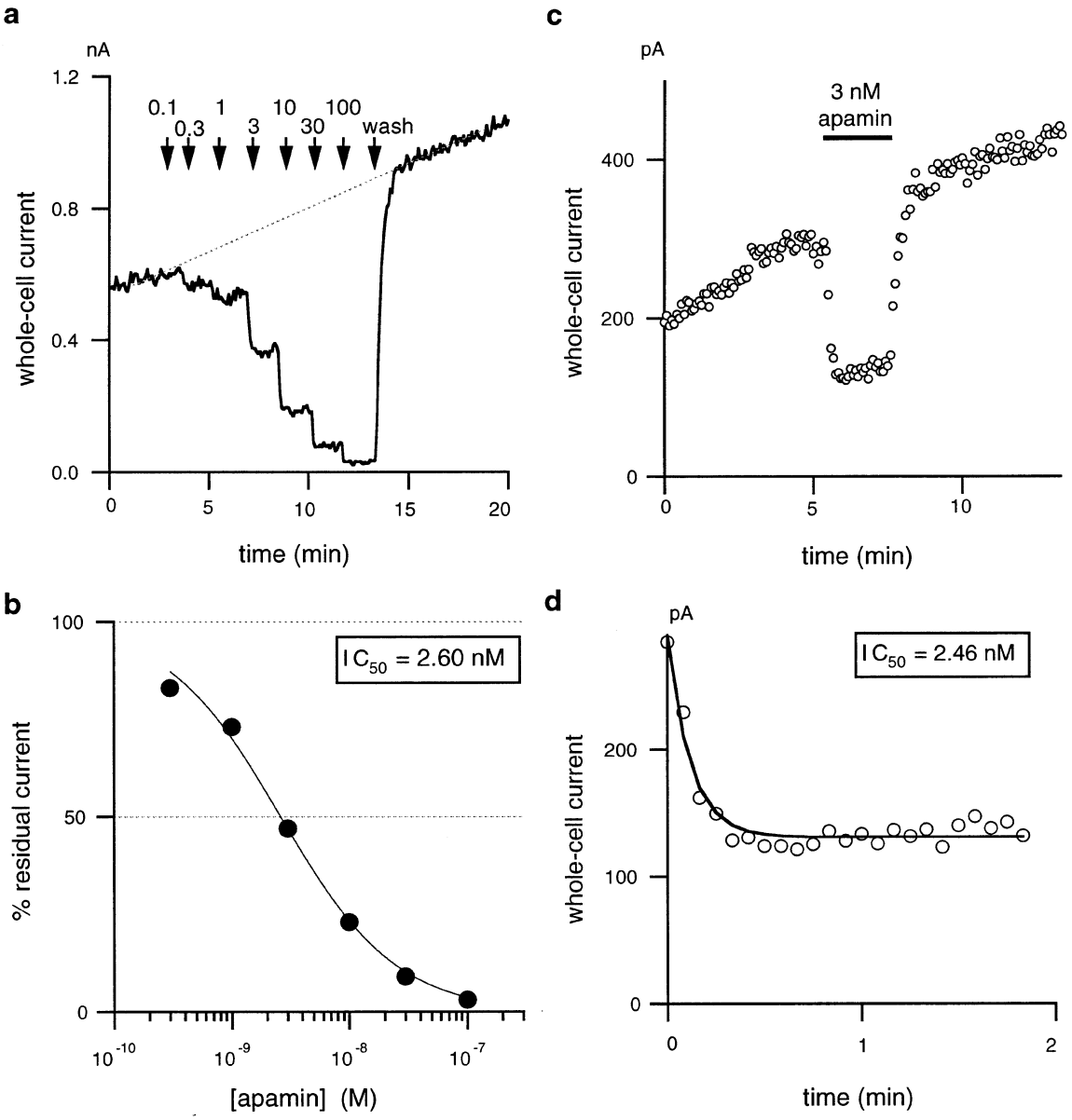

Figure 2 Inhibition of hSK1 by apamin. The inhibition of SK currents were studied in dose-response experiments as the one shown in (a) and in single-dosely experiments as shown in (c). The whole-cell currents measured at +80 mV are plotted as a function of time. In (a) the bath solution was shifted to solutions with the indicated concentrations of apamin at the times marked by arrows and in (c) the presence of 3 nM apamin in the bath solution is indicated by the bar. The dotted line in (a) indicates the estimated baseline during the time of apamin application. (b) and (d) illustrate the calculation of IC_{50} values for the two experiments shown in (a) and (c). In (b) the symbols are the percentage of current remaining plotted as a function of the apamin concentration. The solid curve was obtained after applying a Hill fitting procedure to the data-points. In (d) the symbols are the current measured during application of apamin whereas the curve is the fitted curve obtained from equation (2) in Methods.

blocked by the SK channel blockers tested. Compounds were added once a stable increase in current was obtained which normally was 5–10 min after establishment of the whole-cell configuration. Table 1 summarizes mean values obtained after stable baseline establishment. With 185 nM free calcium in the pipette solution mean currents at −80 mV were about −3 nA whereas currents at +80 mV were close to 500 pA. Values obtained after correction for cell size are listed in the Table, and it is evident that similar levels of current were recorded from hSK1 and rSK2 expressing cells. An inward rectification is illustrated by the ratio of the current at −80 mV and +80 mV. For both subtypes the inward current was 5–6 times larger than the outward current. In addition, the outward current often displayed a negative slope conductance at potentials above +50 mV.

Inhibition of hSK1 by apamin

Figure 2a shows a dose-response experiment with increasing concentrations of apamin applied to a hSK1 expressing cell. The currents measured at +80 mV from the voltage ramps are depicted as a function of time. The bath solution was shifted to apamin-containing solutions (100 pM–100 nM) at the times indicated by the arrows. The dotted line indicates the estimated baseline and the percentage of block was calculated between this baseline and zero current. The percentage of block is shown as a function of the apamin concentration in Figure 2b. The data-points were fitted to a Hill equation (see Methods) and an IC_{50} value of 2.6 nM was obtained in this experiment (mean = 2.50 ± 0.25 nM; $n = 4$) with a Hill coefficient of 0.9. Figure 2c shows the time-course of an experiment with 3 nM apamin present in the bath solution during the time indicated by the bar. Data from the last control point to the last point of apamin application was used to calculate an IC_{50} value from the time course of the block. The data points and the curve obtained by fitting to equation (2) in Methods are shown in Figure 2d. The fitted curve gives an on-rate for apamin of 2.6×10^7 $M^{-1}s^{-1}$, an off-rate of 0.064 s^{-1}, and thus the IC_{50} was 2.46 nM in this experiment. Mean values for on- and off-rates as well as mean IC_{50} values are listed in Table 2. In order to certify that the apamin-sensitivity of hSK1 was not a phenomenon of this particular stable cell line, apamin was tested on HEK 293 and CHO cells transiently transfected with hSK1. In the transiently transfected HEK 293 cells apamin blocked hSK1 with an IC_{50} value of 2.94 ± 0.79 nM ($n = 4$, data not shown) and for the CHO cells an IC_{50} value of 5.13 ± 1.50 nM ($n = 5$, data not shown) was obtained.

Inhibition of rSK2 by apamin

Apamin is a potent blocker of rSK2, and very low concentrations of apamin had to be used in order to construct a full dose-response curve. Figure 3a shows an experiment where apamin blocked rSK2 with an IC_{50} of about 100 pM. At the pM concentrations of apamin applied the block developed slowly and new steady-state levels were not obtained within 3–5 min at each concentration. This slow block development implicates the construction of dose-response curves requires toxin application for more than 5 min for each concentration, which is not acceptable due to the change in baseline current. The time course of the block by 300 pM apamin obtained in another experiment is shown in Figure 3b. By fitting to the time course an IC_{50} value of 75 pM was obtained in this experiment with an on-rate of 4.1×10^7 $M^{-1}s^{-1}$ and an off-rate of 0.003 s^{-1}. These data implicates that apamin has approximately 40 times higher affinity for rSK2 than for hSK1.

Effects of other toxins

A large number of toxins are known to affect ion channels. Taicatoxin is a Ca^{2+}-channel antagonist, that was reported to block the apamin-sensitive K^+ tail-current in rat chromaffin cells at a concentration of 50 nM (Doorty *et al*., 1997). Taicatoxin did, however, neither modify the current through hSK1 or rSK2 channels (100 nM, $n = 3–5$ for each channel subtype, data not shown). Also charybdotoxin, which is a blocker of IK and BK channels, showed no effect on hSK1 and rSK2 (100 nM, $n = 3–5$ at each subtype, data not shown). The scorpion peptide scyllatoxin blocked hSK1 with an IC_{50} value of 80 ± 23 nM ($n = 4$) and rSK2 with an IC_{50} value of 287 ± 13 pM ($n = 4$). Thus the discrimination between the two SK channel subtypes was even stronger for scyllatoxin than observed with apamin.

Effects of small molecule blockers

The plant alkaloid d-tubocurarine is a nicotinic acetylcholine receptor antagonist but it has also been shown to block apamin-sensitive SK channels and AHPs. The concentration-dependent inhibition of hSK1 and rSK2 by d-tubocurarine is depicted in Figure 4. The traces shown are control traces as well as traces after application of the indicated concentrations (in μM) of d-tubocurarine. It appears from the traces that the degree of inhibition is larger at negative membrane potentials

Table 2 Kinetic parameters for the block of hSK1 and rSK2 at +80 mV

Compound	*on-rate* ($M^{-1}s^{-1}$)	*off-rate* (s^{-1})	*IC_{50}*	n
hSK1			3.3 ± 0.91 nM	
Apamin	$1.9 \pm 0.42 \times 10^7$	0.056 ± 0.0067	80 ± 23 nM	5
Scyllatoxin	$3.8 \pm 0.74 \times 10^6$	0.35 ± 0.17	27 ± 11 μM	4
D-tubocurarine	$3.5 \pm 0.93 \times 10^3$	0.082 ± 0.028	762 ± 156 pM	4
UCL 1684	$5.1 \pm 1.5 \times 10^7$	0.031 ± 0.0094	444 ± 121 nM	6
Dequalinium Cl	$1.4 \pm 0.33 \times 10^5$	0.053 ± 0.0061		4
rSK2				
Apamin	$3.7 \pm 0.41 \times 10^7$	0.0033 ± 0.00071	83 ± 13 pM	5
Scyllatoxin	$3.2 \pm 0.30 \times 10^7$	0.0092 ± 0.0012	2 87 ± 13 pM	4
D-tubocurarine	$8.3 \pm 2.2 \times 10^3$	0.14 ± 0.060	17 ± 6.1 μM	4
UCL 1684	$1.3 \pm 0.33 \times 10^8$	0.039 ± 0.0045	364 ± 75 pM	4
Dequalinium Cl	$3.3 \pm 1.3 \times 10^5$	0.044 ± 0.015	162 ± 32 nM	5

The potency of bicuculline methiodide could only be determined in dose-response experiments where IC_{50} values of 15 ± 1.9 μM (hSK1, $n = 4$) and 25 ± 4.0 μM (rSK2, $n = 4$) were obtained. Taicatoxin and charybdotoxin had no effect at 100 nM.

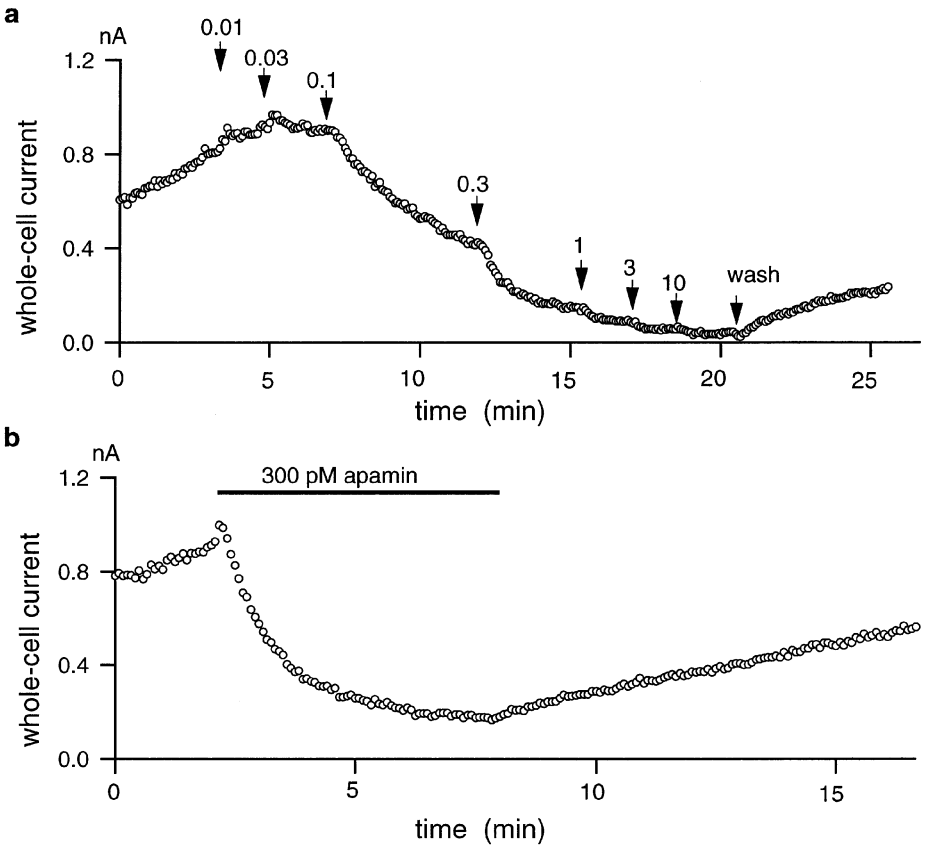

Figure 3 Inhibition of rSK2 by apamin. (a) Dose-response experiment for apamin on a rSK2 expressing HEK 293 cell depicted as the whole-cell current measured at +80 mV as a function of time. The bath solution was changed at the times indicated by the arrows and the values listed are the apamin concentration in the extracellular solution in nM. (b) Current versus time plot for a single-dose experiment in which 300 pM apamin was applied to a rSK2 expressing cell during the time indicated by the bar.

than at positive potentials. This voltage-dependency is clarified in Figure 4c and d where the fraction of current that was blocked by 30 μM d-tubocurarine is plotted as a function of the ramp potential. From these particular dose-response experiments IC_{50} values determined at −80 mV and +80 mV were 17 and 43 μM for hSK1, and 4.6 and 22 μM for rSK2. The mean IC_{50} values found for d-tubocurarine at −80 mV from the kinetical experiments were 12 ± 2 μM for hSK1 and 5 ± 1 μM for rSK2. The values obtained at +80 mV are given in Table 2.

Bicuculline methiodide is a water-soluble $GABA_A$ receptor antagonist that contains a quaternary ammonium. The compound was reported to block the AHP in midbrain, thalamic, and CA1 neurones. We found that the compound blocked hSK1 as well as rSK2 with IC_{50} values of 15 ± 2 μM ($n=4$) and 25 ± 4 μM ($n=3$). These IC_{50} values were determined by constructing dose-response curves since the block developed fast compared to the solution exchange time in the recording chamber. As illustrated in Figure 5, a new equilibrium level of current was obtained at the first point after each drug application and therefore no information was obtained about the on- and off-rates. Bicuculline methiodide was more potent at negative membrane potentials with IC_{50} values at −80 mV of 4.0 ± 0.5 μM (hSK1) and 3.0 ± 0.2 μM (rSK2).

Scientists at University College of London have investigated the structure activity relationship around cyclic dequalinium analogues with UCL 1684 being the most potent blocker synthesized. The compound blocked the AHP in cultured rat sympathetic neurons with an IC_{50} value of approximately 3 nM implicating that UCL 1684 is 100 fold more potent than dequalinium chloride in this preparation. Dequalinium chloride was in the present study found to block the two channel subtypes with almost equal potencies. UCL 1684 was approximately 500 times more potent but also showed little or no difference in the affinity towards the two subtypes. The high affinity for hSK1 implicates that this compound is more potent at hSK1 than apamin. The mean IC_{50} values for dequalinium chloride and UCL 1684 are listed in Table 2.

Discussion and conclusions

Stable expression of hSK1 as well as rSK2 in HEK 239 cells endowed these cells with inward rectifying K^+-selective currents. The ratio of current measured at −80 mV to that at +80 mV was 5–6 for both cell lines, and the IV curves displayed a negative slope at potentials more positive than +50 mV. The currents were strongly Ca^{2+}-dependent as shown by the activation following equilibration with the elevated free Ca^{2+} concentration in the pipette solution. Pipette solutions having a free Ca^{2+} concentration below 100 nM failed to activate the SK currents, whereas free Ca^{2+} concentrations of 185 nM induced currents in the nanoampere range. SK1 as well as SK2 showed sensitivity to apamin, albeit with a 40 fold difference. Scyllatoxin displayed a larger separation of 280 fold between the subtypes, whereas the other compounds showed no pronounced subtype-selectivity despite their high potency.

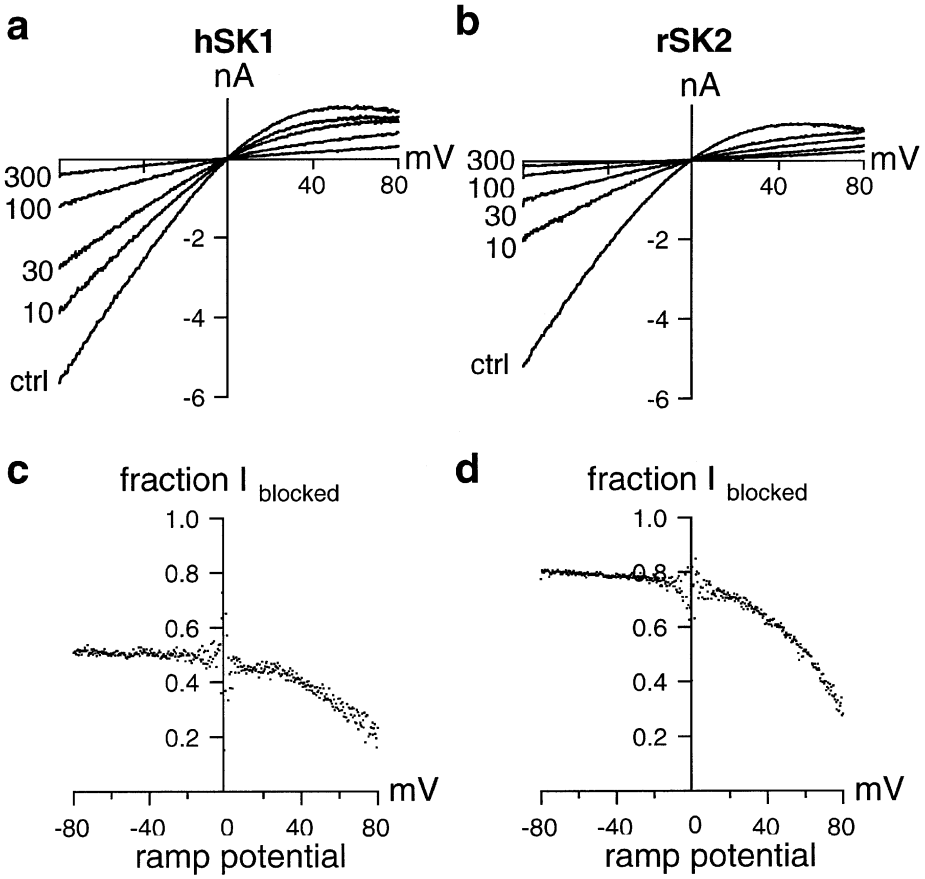

Figure 4 Voltage-dependent block of SK channels by d-tubocurarine. The whole-cell currents as a function of the ramp potential for a hSK1 expressing cell (a) and a rSK2 expressing cell (b). Traces obtained before (ctrl) and after addition of d-tubocurarine at the concentrations indicated (in μM) are shown. The 400 samples recorded during the ramps after block by 30 μM d-tubocurarine were divided by the samples recorded from the corresponding control ramps and these values are depicted as a function of the ramp potential in (c) and (d) to illustrate the voltage-dependency of the block by d-tubocurarine.

Inhibition of the SK channels was characterized in dose-response experiments as well as in single-dose experiments. The dose-response experiments served to select the concentrations to be used in the single-dose experiments and to certify that Michaelis-Menten formalism was valid for the drug-receptor interaction (i.e. that the Hill coefficient was close to 1). The dose-response experiments were useful for most of the blockers, but high-affinity blockers exhibit slow kinetics and the block therefore develops very slowly at low concentrations. The duration of single-dose experiments were shorter, which was of importance due to the sliding baseline. However this experimental design was not useful in the case of bicuculline methiodide since the block developed too fast to be addressed in single-dose experiments. The nature of the continuous shift in baseline (run-up) is not known, but it is somewhat specific for the SK channel-expressing HEK 293 cells, since we do not observe this increase in HEK 293 cells expressing hIK channels (Jensen *et al*., 1998). Interestingly, in inside out patches from *Xenopus* oocytes, rSK2 currents have been shown to display run-down with a mono-exponential time constant of 2.2 min (Ishii *et al*., 1997).

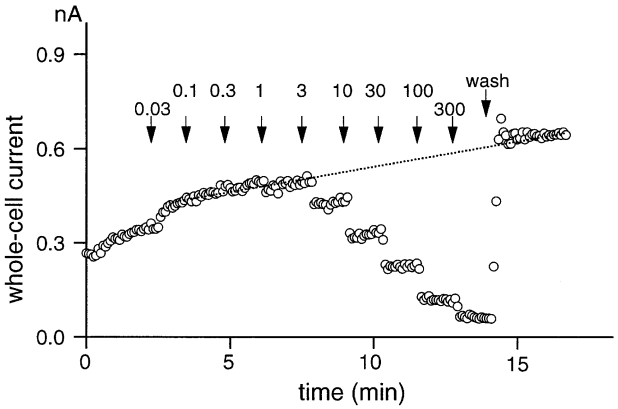

Figure 5 Block of hSK1 by bicuculline methiodide. The fast block of hSK1 current by bicuculline methiodide is shown as a function of time. The bath solutions were changed at the times indicated by arrows and the values are the bicuculline methiodide concentrations in the extracellular solution in μM. The dotted line is the estimated baseline during the time of drug application.

The most surprising finding in the present study is the significant apamin-sensitivity of hSK1, where we have determined an IC_{50} value close to 3 nM for block of hSK1 channels both stably and transiently expressed in HEK 293 cells. The finding is in contrast to the insensitivity to 100 nM apamin observed by Köhler *et al*. (1996) for the channels expressed in *Xenopus* oocytes. The human SK1 channel was used in both studies ruling out any species-related difference in sensitivity. However, the expression system used can have dramatic effects on the pharmacology of ion channels as seen with the block of HERG channels by E-4031 where the IC_{50} value for block is 588 nM in oocytes (Trudeau *et al*., 1995) compared to 7.7 nM in HEK 293 cells (Zhou *et al*., 1998). There are no potential N-linked glycosylation sites in the predicted extracellular domains of hSK1, so differences in

protein glycosylation in the two expression systems are not likely to explain the difference in sensitivity. Other explanations could be related to differentiated regulation by intracellular second messengers in the two systems or perhaps even the presence of a β-subunit. Expression of β-subunits may change the pharmacological properties of ion channels as seen for the dehydrosoyasaponin- and charybdotoxin-sensitivity of the BK channel (McManus *et al*., 1995; Hanner *et al*., 1997) or the sulphunylurea-sensitivity of the K_{ATP} channel (Ämmälä *et al*., 1996). Calmodulin is constitutively bound to the SK channel (Xia *et al*., 1998) and can be regarded as a β-subunit, but it can not be excluded that other unidentified proteins are associated with the SK channels. One difference between the two studies is that Köhler *et al*. (1996) studied apamin block in the presence of 5 μM internal Ca^{2+} whereas we used 185–220 nM Ca^{2+}. This might influence the potency of apamin for SK1, but it is noteworthy that similar potencies were found for SK2 in the two studies.

It is also noteworthy that the IV relation of especially hSK1 expressed in HEK 293 cells show a larger degree of rectification than the currents from oocytes (Köhler *et al*., 1996; Ishii *et al*., 1997). The degree of rectification is often related to intracellular factors and it is possible that the differences in run-up/run-down, rectification and apamin-sensitivity of hSK1 is due to such components being different in oocytes and mammalian cells.

It has been suggested that the SK1 subunits constitute the current underlying the apamin-insensitive sAHP. However, the low nanomolar affinity of apamin for hSK1 expressed in mammalian cells found in this study would argue against at least the human form of this channel subtype being responsible for the sAHP. No biophysical or pharmacological data are available on the rat homologue of SK1. Recent data from CA1 pyramidal cells suggest that the channels underlying the sAHP have gating kinetics which are far slower than those obtained for the homomeric SK1 channels expressed in *Xenopus* oocytes (Sah & Clements, 1999). Further, in a recent paper by Stocker *et al*. (1999) d-tubocurarine as well as bicuculline methochloride were shown to block the apamin-sensitive mAHP in CA1 neurones without affecting the apamin-insensitive sAHP. Based on the present knowledge, that d-tubocurarine and bicuculline do not discriminate between hSK1 and rSK2, it is not likely that the sAHP was mediated by SK1 channels. No pharmacological blockers of the sAHP are known, but the sAHP can be inhibited by stimulation of the cells with a number of neurotransmitters (Schwindt *et al*., 1992; Pedarzani & Storm, 1993) and it still remains possible, that this current is conducted by an as yet unrecognized type of Ca^{2+}-sensitive K^+ channel.

D-tubocurarine is an inhibitor of the nicotinic acetylcholine receptor, but it also blocks SK channels. In this study we find that SK1 and SK2 channels are both blocked, and that the difference in IC_{50} values between the two subtypes is 2–3 fold, which is significantly less than the 30–65 fold difference found in the *Xenopus* oocyte experiments (Köhler *et al*., 1996; Ishii *et al*., 1997). As for the data with apamin, the IC_{50} values found at rSK2 are comparable in the two studies, whereas the potency of d-tubocurarine at hSK1 is higher in the HEK 293 cells than in *Xenopus* oocytes. The block by d-tubocurarine was voltage-dependent with the effect being weaker at positive potentials. The reason for this voltage-dependency could be that curare, which binds in the outer mouth of the channel pore (Ishii *et al*., 1997) and has a relatively weak affinity for the receptor, is knocked off by the K^+ ions flowing out of the channel. Bicuculline methiodide showed the same type of voltage-dependent block as d-tubocurarine.

The 31 amino acid polypeptide scyllatoxin originates from the toxin of the scorpion *Leiurus quinquestriatus hebraus* (Chicchi *et al*., 1988; Auguste *et al*., 1990). In this study scyllatoxin has proved to be the molecule which most clearly discriminates between the two SK channel subtypes and it is thus the most useful compound to address the involvement of SK channel subtypes in functional responses.

Dequalinium chloride bears some of the same pharmacophore as d-tubocurarine and apamin which are two quaternary amino-groups with a separation of 11-14 Å. UCL 1684 is a cyclic analogue of dequalinium in which the distance between the charges has been fixed strongly, and this has increased the potency of the compound as blocker of the AHP in sympathetic neurones 100 fold (Campos-Rosa *et al*., 1998). In the present study UCL 1684 was found not to discriminate between the two SK channel subtypes despite the fact that it has a potency which is comparable to that of apamin and scyllatoxin on SK2 channels. At SK1 channels UCL 1684 is the most potent blocker described. Thus, for a blocker to discriminate between the two SK channel subtypes it is not sufficient to be potent and have an apamin-like structure.

In conclusion, potent blockers of SK channels have been used in a large number of studies on native tissues to address the function of these channels. Some of the blockers show SK channel subtype-selectivity, but the separation between the subtypes is different when studied on cloned channels expressed in mammalian cells as compared to *Xenopus* oocytes. We have here performed a detailed characterization of a number of peptides and small molecule blockers on cloned SK1 and SK2 channels expressed in HEK 293 cells. Three molecules exhibited pM potencies for SK2, and their sensitivity for SK1 was lower by factors of 280 fold (scyllatoxin), 40 fold (apamin) and 2 fold (UCL 1684). One specific implication of the study is, that the current mediating the slow after-hyperpolarization in neurones is not likely to be conducted by SK1 channels.

The work was supported by EU grant no. BMH4-CT-97-2118 to SPO. The excellent technical assistance offered by Jette Sonne and Lene Gylle Larsen is gratefully acknowledged.

References

ÄMMÄLÄ, C., MOORHOUSE, A., GRIBBLE, F., ASHFIELD, R., PROKS, P., SMITH, P.A., SAKURA, H., COLES, B., ASHCROFT, S.J.H. & ASHCROFT, F.M. (1996). Promiscuous coupling between the sulphonylurea receptor and inwardly rectifying potassium channels. *Nature,* **379,** 545–548.

AUGUSTE, P., HUGUES, M., GRAVE, B., GRESQUIERE, J.C., MAES, P., TARTAR, A., ROMEY, G., SCHWEITZ, H. & LAZDUNSKI, M. (1990). Leirotoxin I (Scyllatoxin), a peptide ligand for Ca^{2+}-activated K^+ channels. *J. Biol. Chem.,* **256,** 4753–4759.

BLATZ, A.L. & MAGLEBY, K.L. (1986). Single apamin-blocked Ca-activated K^+ channels of small conductance in cultured rat skeletal muscle. *Nature,* **323,** 718–720.

CAMPOS-ROSA, J., DUNN, P.M., GALANAKIS, D., GANELLIN, C.R., JENKINSON, D.H. & YANG, D. (1997). World Patent Application, WO 97/48705.

CAMPOS-ROSA, J., GALANAKIS, D., GANELLIN, C.R., DUNN, P.M. & JENKINSON, D.H. (1998). Bis-quinolinium Cyclophanes: 6,10-Diaza - 3(1,3) 8 (1,4) - dibenzena - 1,5(1,4) - diquinolinacyclodecaphane (UCL 1684), the first nanomolar, non-peptidic blocker of the apamin-sensitive Ca^{2+}-activated K^+ channel. *J. Med. Chem.,* **41,** 2 – 5.

CASTLE, N.A., HAYLETT, D.G., MORGAN, J.M. & JENKINSON, D.H. (1993). Dequalinium: a potent inhibitor of apamin-sensitive K^+ channels in hepatocytes and of nicotinic responses in skeletal muscle. *Eur. J. Pharmacol.,* **236,** 201 – 207.

CHICCHI, G.G., GIMENEZ-GALLEGO, G., BER, E., GARCIA, M.L., WINQUIST, R. & CASCIERI, M.A. (1988). Purification and characterization of a unique, potent inhibitor of apamin binding from *Leiurus quinquestriatus hebraeus* venom. *J. Biol. Chem.,* **263,** 10192 – 10197.

DEBARBIEUX, F., BRUNTON, F. & CHARPAK, S. (1998). Effect of bicuculline on thalamic activity: A direct blockade of I_{AHP} in reticularis neurons. *Am. Physiol. Soc.,* **79,** 2911 – 2918.

DOORTY, K.B., BEVAN, S., WADSWORTH, J.D.F. & STRONG, P.N. (1997). A novel small conductance Ca^{2+}-activated K^+ channel blocker from oxyuranus scutellatus taipan Venom. *J. Biol. Chem.,* **32,** 19925 – 19930.

DUNN, P.M. (1994). Dequalinium, a selective blocker of the slow afterhyperpolarization in rat sympathetic neurons in culture. *Eur. J. Pharmacol.,* **252,** 189 – 194.

GOH, J.W. & PENNEFATHER, P.S. (1987). Pharmacological and physiological properties of the after-hyperpolarization current of bullfrog ganglion neurones. *J. Physiol. (Lond.),* **394,** 315 – 330.

HABERMANN, E. (1984). Apamin. *Pharmac. Ther.,* **25,** 255 – 270.

HANNER, M., SCHMALHOFER, W.A., MUNUJOS, K., KNAUS, H.G. & GARCIA, M.L. (1997). The beta subunit of the high-conductance calcium-activated potassium channel contributes to the high-affinity receptor for charybdotoxin. *Proc. Natl. Acad. Sci. U.S.A.,* **94,** 2853 – 2858.

HANSELMANN, C. & GRISSMER, S. (1996). Characterization of apamin-sensitive Ca^{2+}-activated potassium channels in human leukaemic T lymphocytes. *J. Physiol. (Lond.),* **496.3,** 627 – 637.

ISHII, T.M., MAYLIE, J. & ADELMAN, J.P. (1997). Determinants of apamin and d-tubocurarine block in SK potassium channels. *J. Biol. Chem.,* **37,** 23195 – 23200.

JENSEN, B.S., STRØBAEK, D., CHRISTOPHERSEN, P., JØRGENSEN, T.D., HANSEN, C., SILAHTAROGLU, A., OLESEN, S.-P. & AHRING, P.K. (1998). Characterization of the cloned human intermediate-conductance Ca^{2+}-activated K^+ channel. *Am. J. Physiol.,* **275,** C850 – C856.

JOHNSON, S.W. & SEUTIN, V. (1997). Bicuculline methiodide potentiates NMDA-dependent burst firing in rat dopamine neurons by blocking apamin-sensitive Ca^{2+}-activated K^+ currents. *Neurosci. Lett.,* **231,** 13 – 16.

KÖHLER, M., HIRSCHBERG, B., BOND, C.T., KINZIE, J.M., MARRION, N.V., MAYLIE, J. & ADELMAN, J.P. (1996). Small-conductance, calcium-activated potassium channels from mammalian brain. *Science,* **273,** 1709 – 1714.

MCMANUS, O.B., HELMS, L.M.H., PALLANCK, L., GANETZKY, B. & SWANSON, R. (1995). Functional role of the β subunit of high conductance calcium-activated potassium channels. *Neuron,* **14,** 645 – 650.

MESSIER, C., MOURRE, C., BONTEMPI, B., SIF, J., LAZDUNSKI, M. & DESTRADE, C. (1991). Effect of apamin, a toxin that inhibits Ca^{2+}-dependent K^+ channels, on learning and memory processes. *Brain Res.,* **551,** 322 – 326.

NOHMI, M. & KUBA, K. (1984). (+)-Tubocurarine blocks the Ca^{2+}-dependent K^+-channel of the bullfrog sympathetic ganglion cell. *Brain Res.,* **301,** 146 – 148.

PEDARZANI, P. & STORM, J.F. (1993). PKA mediates the effects of monoamine transmitters on the K^+ current underlying the slow spike frequency adaptation in hippocampal neurons. *Neuron,* **11,** 1023 – 1035.

PENNEFATHER, P., LANCASTER, B., ADAMS, P.R. & NICOLL, R.A. (1985). Two distinct Ca-dependent K currents in bullfrog sympathetic ganglion cells. *Proc. Natl. Acad. Sci. U.S.A.,* **82,** 3040 – 3044.

SAH, P. (1995). Properties of channels mediating the apamin-insensitive afterhyperpolarization in vagal motoneurons. *J. Neurophysiol.,* **74,** 1772 – 1776.

SAH, P. (1996). Ca^{2+}-activated K^+ currents in neurones: types, physiological roles and modulation. *Trends Neurosci.,* **19,** 150 – 154.

SAH, P. & CLEMENTS, J.D. (1999). Photolytic manipulation of $[Ca^{2+}]_i$ reveals slow kinetics of potassium channels underlying the afterhyperpolarization in hippocampal pyramidal neurons. *J. Neurosci.,* **19,** 3657 – 3664.

SAH, P. & MCLACHLAN, E.M. (1991). Ca^{2+}-activated K^+ currents underlying the afterhyperpolarization in guinea pig vagal neurons: A role for Ca^{2+}-activated Ca^{2+} release. *Neuron,* **7,** 257 – 264.

SCHWINDT, P.C., SPAIN, W.J. & CRILL, W.E. (1992). Calcium-dependent potassium currents in neurons from cat sensorimotor cortex. *J. Neurophysiol.,* **67,** 216 – 226.

SCHWINDT, P.C., SPAIN, W.J., FOEHRING, R.C., STAFSTROM, C.E., CHUBB, M.C. & CRILL, W.E. (1988). Multiple potassium conductances and their functions in neurons from cat sensorimotor cortex in vitro. *J. Neurophysiol.,* **59,** 424 – 449.

STOCKER, M., KRAUSE, M. & PEDARZANI, P. (1999). An apamin-sensitive Ca^{2+}-activated K^+ current in hippocampal pyramidal neurons. *Proc. Natl. Acad. Sci. U.S.A.,* **96,** 4662 – 4667.

STORM, J.F. (1987). Action potential repolarization and a fast after-hyperpolarization in rat hippocampal pyramidal cells. *J. Physiol.,* **385,** 733 – 759.

TRUDEAU, M.C., WARMKE, J.W., GANETZKY, B. & ROBERTSON, G.A. (1995). HERG, a human inward rectifier in the voltage-gated potassium channel family. *Science,* **269,** 92 – 95.

VERGARA, C., LATORRE, R., MARRION, N.V. & ADELMAN, J.P. (1998). Calcium-activated potassium channels. *Curr. Opin. Neurobiol.,* **8,** 321 – 329.

XIA, X.-M., FAKLER, B., RIVARD, A., WAYMAN, G., JOHNSON-PAIS, T., KEEN, J.E., ISHII, T., HIRSCHBERG, B., BOND, C.T., LUTSENKO, S., MAYLIE, J. & ADELMAN, J.P. (1998). Mechanism of calcium gating in small-conductance calcium-activated potassium channels. *Nature,* **395,** 503 – 507.

ZHOU, Z., GONG, Q., YE, B., FAN, Z., MAKIELSKI, J.C., ROBERTSON, G.A. & JANUARY, C.T. (1998). Properties of HERG channels stably expressed in HEK 293 cells studied at physiological temperature. *Biophys. J.,* **74,** 230 – 241.

(Received July 12, 1999
Accepted November 26, 1999)